JOURNAL OF THEORETICAL AND APPLIED MECHANICS
56, 1, pp. 203-212, Warsaw 2018
DOI: 10.15632/jtam-pl.56.1.203

STEADY AND UNSTEADY ANALYSIS OF NACA 0018 AIRFOIL IN VERTICAL-AXIS WIND TURBINE

Krzysztof Rogowski
Warsaw University of Technology, Institute of Aeronautics and Applied Mechanics, Warsaw, Poland
e-mail: krogowski@meil.pw.edu.pl

Martin O.L. Hansen
Technical University of Denmark, DTU Wind Energy, Department of Wind Energy, Lyngby, Denmark
e-mail: molh@dtu.dk

Ryszard Maroński
Warsaw University of Technology, Institute of Aeronautics and Applied Mechanics, Warsaw, Poland
e-mail: maron@meil.pw.edu.pl

Numerical results are presented for aerodynamic unsteady and steady airfoil characteristics of the NACA 0018 airfoil of a two-dimensional vertical-axis wind turbine. A geometrical model of the Darrieus-type wind turbine and the rotor operating parameters used for numerical simulation are taken from the literature. Airfoil characteristics are investigated using the same mesh distribution around the airfoil edges and two turbulence models: the RNG k-ε and the SST Transition. Computed results for the SST Transition model are in good agreement with the experiment, especially for static airfoil characteristics.

Keywords: airfoil characteristics, vertical-axis wind turbine, computational fluid dynamics

1. Introduction

Generally, with respect to the orientation of the rotor shaft, wind turbines can be divided into two main groups: horizontal-axis wind turbines (HAWTs, or axial flow turbines) and vertical-axis wind turbines (VAWTs, or cross-flow turbines) (Maroński, 2016). Wind turbines can also be divided with respect to the principle of operation: lift-driven and drag-driven machines (Rogowski, 2014). Although, HAWTs are now widely used in the industry, large-scale VAWTs are designed as offshore units – floating wind turbines (Madsen *et al.*, 2013; Borg *et al.*, 2014). Aerodynamic efficiency (power coefficient) of drag-driven wind turbines is low, therefore, they are used relatively rarely (Rogowski and Maroński, 2015). In 1931, Georges J.M. Darrieus, a French aeronautical engineer, patented his invention – a new type of windmill designed for power generation (Blackwell, 1974). The Darrieus wind turbine is a lift-driven wind turbine having two or more blades. The rotor of the Darrieus wind turbine can achieve relatively high aerodynamic efficiency (Hau, 2006). Originally, the Darrieus wind turbine had curved blades with a symmetrical airfoil in their cross sections. The curved blade shape, so-called troposkien, was designed to avoid large bending stresses of the blades, especially when applied to large units (Paraschivoiu, 2009). Darrieus-type wind turbines are designed both as large- and small-size wind turbines with both curved and straight blades. The characteristics of the Darrieus-type wind turbines are: slightly lower power coefficient than HAWTs (Amet *et al.*, 2009); the gearbox and the power generator can be installed at the ground level; the yaw system is not needed because the rotor operates regardless of the wind direction. The main shortcomings of these wind turbines are: low starting torque and vibrations of the structure during rotor operation

(Paraschivoiu, 2009). The growing demand for decentralized electricity generation in urban and rural areas is the motivation for studying wind turbines in a small scale.

Darrieus-type vertical-axis wind turbines are relatively simple devices. The movement of a single wind turbine blade is similar to the movement of the pitching blade. During rotation of the rotor, the blade angle of attack, the local Reynolds number and the relative wind velocity vary according to the rotor azimuthal angle. These variations also depend on the relationship between the tangential velocity of the wind turbine blade and wind velocity. For these reasons, many nonlinear phenomena occur in a single cycle of the blade (Laneville and Vittecoq, 1986). The rotor power coefficient defined as the ratio of the power absorbed by the rotor shaft divided by the power available from the air stream flowing through the rotor swept area (Hansen, 2008), depends on the tip speed ratio defined as the ratio of the tangential blade velocity to the wind speed. Typical Darrieus wind turbine achieves the maximum power coefficient of about 0.4 at the tip speed ratio of 5-6 (Hau, 2006). Dynamic effects associated with dynamic stall phenomena occur at low tip speed ratios (below 4). Aerodynamic effects of the rotor elements such as blades, tower, struts, etc., play important role in reduction of the rotor power coefficient at high tip speed ratios (above 6) (Paraschivoiu, 2009).

Although, measurement techniques have been improved in the recent years, only a few experimental tests of unsteady aerodynamic blade loads have been performed. Measurement difficulties are particularly associated with the tangential blade load component (tangential to the rotor swept area) which is responsible for creation of the rotor torque. This is because the tangential blade load is very low compared with the normal blade load component (normal to the rotor swept area). Experiments referring to aerodynamic blade loads of the Darrieus-type vertical-axis wind turbines were performed in a water towing tank at Texas Tech University (Strickland *et al.*, 1979, 1981). Laneville and Vittecoq (1986) conducted investigations of lift and drag airfoil characteristics of a small-size vertical-axis Darrieus-type wind turbine in a wind tunnel. Ferreira *et al.* (2011) showed that it was possible, though crudely, that the blade loading could be extracted from velocity flow fields using a method that they had developed.

Streamtube models and single-wake vortex models are often used in simulations of aerodynamic blade loads of VAWTs (Paraschivoiu, 2009; Ferreira, 2009). Nowadays, computational methods of fluid dynamics (CFD) have become popular in many areas of engineering as they can provide very accurate results when referring to the experiments performed on a full-scaled object (Lichota, 2013; Lichota, 2016). The incorporated turbulence models are in numerical computations a compromise between the available hardware capabilities and accuracy of computations. In order to resolve all scales of turbulence, it is necessary to apply an appropriate mesh with very small grid elements. Using a space-time mesh fine enough to compute all scales of turbulence is still a very difficult task for modern supercomputers. However, the increase in computing power of modern computers has led to the development of computationally expensive turbulence models (Ferreira *et al.*, 2007). Ponta and Jacovkis (2001) investigated the Darrieus-type wind turbine using a combined method consisting of a classic free vortex model and finite element techniques. Amet *et al.* (2009) performed CFD analysis of the two-bladed rotor basing on the experiment of Laneville and Vittecoq (1986) at tip speed ratios of 2 and 7. Many numerical simulations of two-dimensional Darrieus-type wind turbines using different turbulence models were made by Rogowski (2014). 3D simulations of a straight-bladed vertical axis tidal turbines were performed by Marsh *et al.* (2013) using the SST k-ω turbulence model.

Generally, Darrieus wind turbines operate at low Reynolds numbers. The range of the blade angle of attack is very large. Streamtube models and vortex models require C_L and C_D airfoil characteristics in order to compute aerodynamic blade loads. Aerodynamic characteristics can be computed using CFD methods (Rogowski, 2014; Sarlak *et al.*, 2014) or performed experimentally (Sheldahl and Klimas, 1981; Laneville and Vittecoq, 1986).

The three main objectives of this work are as follows:

- Determination of aerodynamic coefficients for unsteady flow around the wind turbine using a hybrid mesh consisting of a structured quadrilateral mesh close to airfoil edges and an unstructured triangle mesh elsewhere.
- Investigation of steady characteristic of the NACA 0018 airfoil using the same mesh distribution as during the unsteady flow simulation of the VAWT.
- Comparison of the aerodynamic characteristics for two turbulence models: the RNG k-ε and the SST Transition.

2. Wind turbine parameters

In this paper, the authors present computed airfoil characteristics of a rotating wind turbine blade and of a stationary airfoil. Computed airfoil characteristics are compared with the experiment of Laneville and Vittecoq (1986). The experiment was conducted in an open jet wind tunnel at the Universite de Sherbrooke. The main objective of Laneville and Vittecoq was to measure aerodynamic blade loads for a two-bladed rotor with zero offset pitch angle using strain gauges. Basic geometrical parameters of the investigated wind turbine are given in Table 1. In the central part of the rotor, a torsion-free steel shaft supported by two ball bearings was mounted. The rotor blades made of balsa wood were supported by horizontal arms at the lower part of the rotor and by two guitar wires stretched between the shaft and the blades at the upper part of the rotor. Measuring devices such as force transducers and amplifiers were placed in the lower horizontal arms. During the experiment, a special variable-speed electric motor was used to maintain the correct rotational velocity. The effect of centrifugal forces on aerodynamic blade loads were removed from experimental data. The experimental measured data was not corrected for blockage effects. The method of measurement of aerodynamic blade load components is presented in Fig. 1.

Table 1. Basic parameters of the investigated wind turbine

Parameter	Value
Rotational speed n [rpm]	300
Rotor radius R [m]	0.3
Chord c [m]	0.061
Airfoil	NACA 0018
Number of blades N	2
Tower diameter d [m]	0.0381
Tip speed ratio TSR	5
Wind velocity V_∞ [m/s]	1.88

The static NACA 0018 airfoil characteristics C_L and C_D were measured in the experiment using the same wind turbine and using the same measuring system as described above (Laneville and Vittecoq, 1986).

3. Lift and drag coefficients

In this paper, the angle of attack is an angle between the tangential velocity of the rotor blade V_T ($V_T = \omega R$, where ω is angular velocity of the rotor, R – rotor radius) and relative velocity V_R which is a resultant of the wind speed V_∞ and the tangential velocity V_T taken with the minus sign (Fig. 2)

$$\mathbf{V}_R = \mathbf{V}_\infty - \mathbf{V}_T \tag{3.1}$$

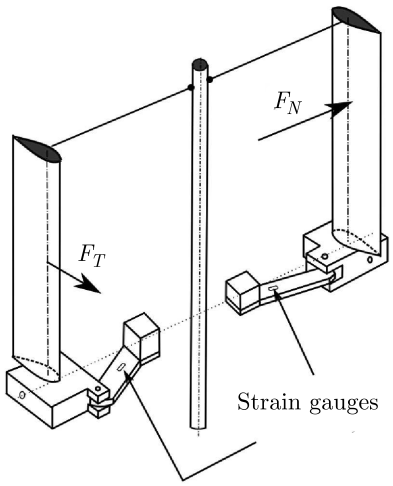

Fig. 1. Silhouette of the turbine rotor and the method of measurement of aerodynamic blade loads (Laneville and Vittecoq, 1986)

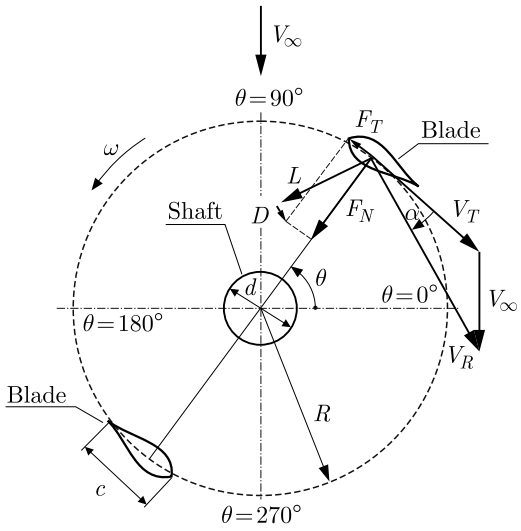

Fig. 2. Geometrical parameters of the rotor. Velocity vectors, angles and aerodynamic loads

From geometrical considerations (Fig. 2), the vector components V_R in the tangential and normal directions to the blade trajectory are respectively

$$V_{Rt} = V_T + V_\infty \cos\theta \qquad V_{Rn} = V_\infty \sin\theta \tag{3.2}$$

where θ is the azimuth angle. The tangent angle of attack α is

$$\tan\alpha = \frac{V_{Rn}}{V_{Rt}} = \frac{V_\infty \sin\theta}{V_T + V_\infty \cos\theta} \tag{3.3}$$

Dividing the numerator and denominator of this equation by V_∞ we get

$$\tan\alpha = \frac{\sin\theta}{\frac{V_T}{V_\infty} + \cos\theta} \tag{3.4}$$

TSR is the tip speed ratio defined as

$$TSR = \frac{V_T}{V_\infty} = \frac{\omega R}{V_\infty} \tag{3.5}$$

Taking into account the above formula in equation (3.4), the angle of attack is

$$\alpha = \tan^{-1}\Big(\frac{\sin\theta}{\cos\theta + TSR}\Big) \tag{3.6}$$

The relative velocity V_R can be defined as

$$V_R = \sqrt{(\omega R + V_\infty \cos\theta)^2 + (V_\infty \sin\theta)^2} \tag{3.7}$$

During wind turbine operation, the blade angle of attack varies with the azimuth θ, whereas the relative wind velocity is associated with a variation in the angle of attack (Fig. 3). The lift and drag coefficients are given by

$$C_L = \frac{L}{\frac{1}{2}\rho c(\omega R)^2} \qquad C_D = \frac{D}{\frac{1}{2}\rho c(\omega R)^2} \tag{3.8}$$

where L is the lift force, D – drag, ρ – air density, c – chord.

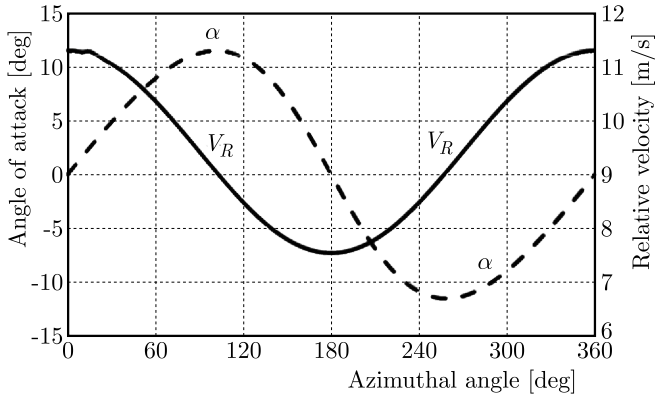

Fig. 3. Evolution of the angle of attack and the relative velocity vs azimuthal angle at the tip speed ratio of 5

The definitions of the lift and drag coefficients contain the tangential velocity of the blade $V_T = \omega R$ instead of the relative velocity V_R. In the case of VAWTs, the relative velocity is constantly changing in both magnitude and incidence. The use of the constant reference velocity in the dynamic pressure is desirable since it is possible to compare force coefficients for different airfoils (Danao *et al.*, 2012; Amet *et al.*, 2009).

4. Numerical model

One of the main objectives of this study is to investigate unsteady aerodynamic characteristics of the wind turbine airfoil and steady aerodynamic characteristics of the same airfoil. The numerical two-dimensional model of the vertical-axis Darrieus-type wind turbine consists of two NACA 0018 airfoils and a tower which has been modeled as a circle (Fig. 2). Simulations of the steady airfoil characteristics have been performed using only a single NACA 0018 airfoil with the same chord.

The model of the wind turbine rotor has been enclosed in a square area of a virtual wind tunnel. According to the previous investigations of the authors (Rogowski, 2014; Rogowski and Maroński, 2015), the length of the virtual wind tunnel should be at least equal to ten rotor diameters. The static characteristics of NACA 0018 have been obtained using one airfoil placed in a square area of the virtual wind turbine with the same length as in the case of the rotating rotor.

The mesh near airfoils has been created using structural quadrilateral elements. The height of the first layer of the structural grid is $7 \cdot 10^{-7}$ m giving $y^+ \leqslant 1$. The growth rate of each layer of the structured mesh is 1.13. The airfoil edges are divided into small parts with lengths of $2 \cdot 10^{-4}$ m. The growth rate of the unstructured mesh is 1.06. The mesh for unsteady simulations, presented in Fig. 4 contains of 133 366 elements. In the case of the stationary airfoil, the same mesh distribution around the NACA 0018 is used and the number of mesh elements of the virtual wind tunnel is 74 834.

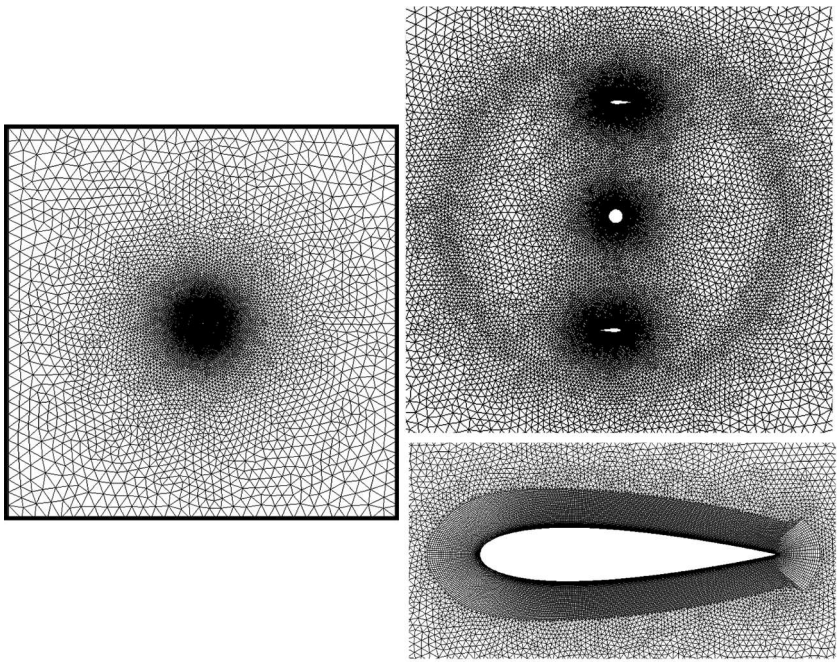

Fig. 4. Mesh distribution

In this paper, two turbulence models are taken into account: the two-equation RNG k-ε and the four-equation SST Transition. The RNG k-ε turbulence model closes the average Navier-Stokes equations introducing two transport equations: one for turbulent kinetic energy and one for turbulent dissipation. The SST Transition turbulence model solves the transport equations for the turbulence kinetic energy, the specific dissipation rate, the intermittency and the transition onset criteria. More detailed description of these turbulence models can be found in the ANSYS, Inc.15.0 documentation.

Turbulence parameters of the wind tunnel of the Universite de Sherbrooke are unknown. However, in the case of open jet wind tunnels, the turbulence intensity of the incoming flow is usually high. Therefore, in this simulation, the value of the turbulence intensity is assumed to be 5%.

5. Results

5.1. Unsteady airfoil characteristics of the wind turbine blade

Figures 5a and 5b present drag and lift coefficients as functions of the angle of attack. The airfoil characteristics are computed using two turbulence models: the RNG k-ε and the SST Transition. The numerical results are compared with the experiment of Laneville and Vittecoq (1986). As it can be seen from Figs. 5a and 5b, the computed results of the drag coefficients are more similar to the experimental results than in the case of the lift coefficient. The differences can be caused by the accuracy of measuring devices. According to Laneville and Vittecoq (1986), with the increasing tip speed ratio, the precision of experimental data decreases, especially for

the lift coefficient. The precision of experimental data has been estimated as follows: $C_D \pm 5\%$ and $C_L \pm 12\%$. Even though the experiment was considered as a two-dimensional (large aspect ratio of the blades), the 3D aerodynamic effects such as tip vortices can reduce the efficiency of the device (Paraschivoiu, 2009; Scheurich *et al.*, 2011). Analyzing the obtained numerical results of airfoil characteristics, hysteresis loops both of the lift and drag coefficients are visible (Figs. 5a and 5b). In the upwind part of the rotor, for the azimuth from 0 deg to 90 deg, a significant increase in the lift and drag coefficients can be observed. Moreover, at the azimuthal angle of zero, which corresponds to the zero angle of attack, the lift coefficients are 0.23 and 0.37 for the SST Transient and the RNG k-ε turbulence models, respectively. The non-zero value of the lift force may have several reasons. Firstly, the definition of the angle of attack assumed in this paper does not take into account effects associated with the slowdown of the flow close to the rotor. Secondly, during rotation of the rotor the virtual camber of the airfoil occurs at the zero angle of attack caused by curved flow around the rotor blade. This means that the symmetrical airfoil of the vertical-axis wind turbine behaves as a cambered airfoil (Akimoto *et al.*, 2013). Moreover, in the case of the airfoil oscillating around the zero average angle of attack, C_L cannot be equal to zero because of the momentum and the inertia of the fluid (Laneville and Vittecoq, 1986). With the increasing azimuth from 90 deg to 180 deg, the lift and the drag force coefficients decrease. In the downwind part of the rotor, the computed lift coefficients are still positive while experimental results are negative. The values of the lift force coefficients obtained by the SST Transition turbulence model are much better compared with the RNG k-ε turbulence model.

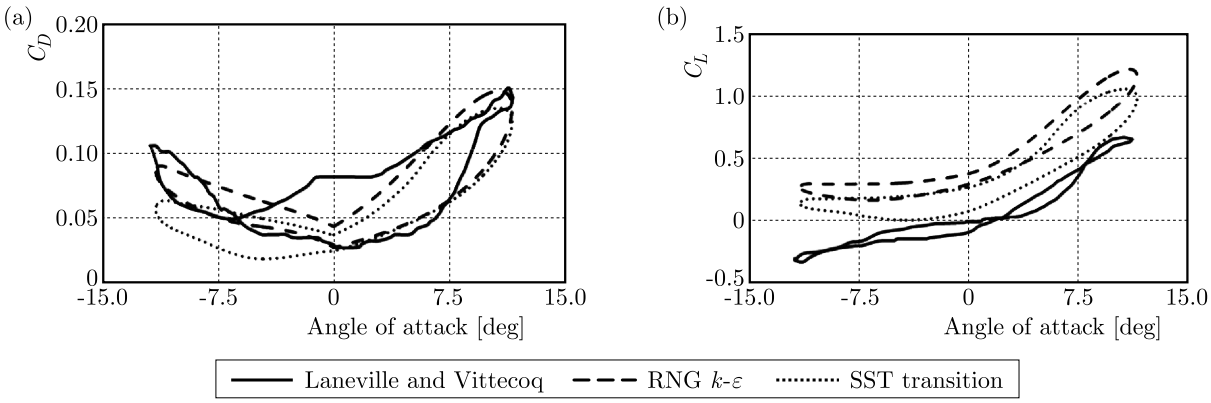

Fig. 5. (a) Drag and (b) lift force coefficient versus the angle of attack at *TSR* of 5

Figure 6 presents vorticity fields computed using the SST Transition turbulence model at three azimuth positions: 0 deg, 60 deg and 120 deg. Analyzing these figures, it can be noticed that at the azimuthal angle of 0 deg two interactions between the blades and the aerodynamic wake occur. At the azimuth of 120 deg, the rotor blade located at the downwind part of the rotor interacts also with the aerodynamic wake from the rotor shaft.

5.2. Airfoil characteristics of NACA 0018

The second part of this paper concerns the analysis of static airfoil characteristics using the same mesh distribution close to the airfoil and the same turbulence models as during unsteady analysis. The obtained results of aerodynamic loads are compared with the experimental data taken from two independent sources (Laneville and Vittecoq, 1986; Sheldahl and Klimas, 1981). The experimental data from the report of Sheldahl and Klimas (1981) are commonly used in simplified aerodynamic models for Darrieus vertical-axis wind turbines applications. The experiments were performed for the Reynolds numbers of $3.8 \cdot 10^4$ in the Laneville and Vittecoq experiment (1986) and $4 \cdot 10^4$ in the experiment of Sheldahl and Klimas (1981).

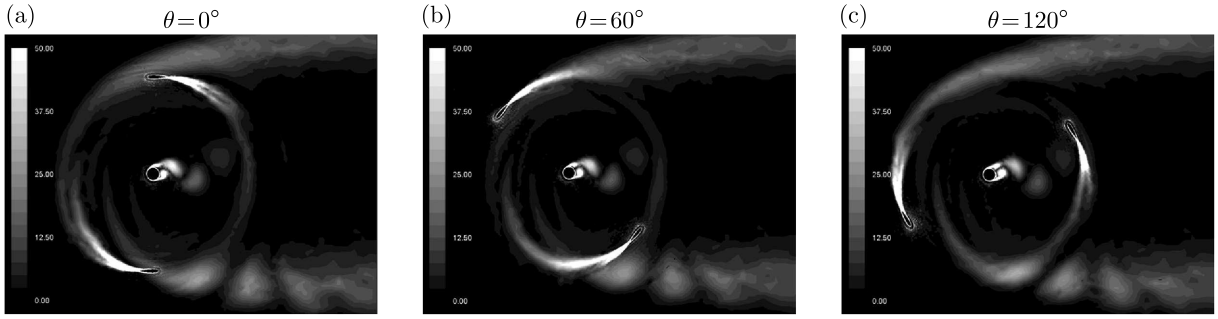

Fig. 6. Evolution of the vorticity field, ω [1/s] – the SST Transition model

The results of aerodynamic force coefficients as a function of the angle of attack are presented in Figs. 7a and 7b. The aerodynamic derivatives $\partial C_L/\partial\alpha$ at the angle of attack range between 0 deg and 5 deg are: 6.0144 for the SST Transition model; 5.78 for the RNG k-ε turbulence model; 6.19 for the experiment of Laneville and Vittecoq (1986) and 4.72 for the experiment of Sheldahl and Klimas (1981). The maximum values of C_L are: 0.71 at the angle of attack of 8.57 deg for the experiment of Laneville and Vittecoq; 0.473 at the angle of attack of 6 deg for the experiment of Sheldahl and Klimas; 0.91 at the angle of attack of 12.5 deg for the SST Transition model and 1.22 at the angle of attack of 15 deg for the RNG k-ε model. The minimum values of the drag coefficient at the zero angle of attack are: 0.034 for the experiment of Laneville and Vittecoq; 0.0214 for the experiment of Sheldahl and Klimas; 0.042 for the SST Transition model and 0.032 for the RNG k-ε model. The largest difference of C_L data between all data series (Fig. 7b) is observed in the static-stall region. Lower drag coefficients by Sheldahl and Klimas (1981) in comparison with those by Laneville and Vittecoq (1986) can be caused by turbulence parameters of the wind tunnel. It is worth noting that the characteristics, both the lift and the drag coefficients, obtained using the SST Transition turbulence model are more comparable with the experimental results of Laneville and Vittecoq (1986) than the experimental results of Sheldahl and Klimas (1981).

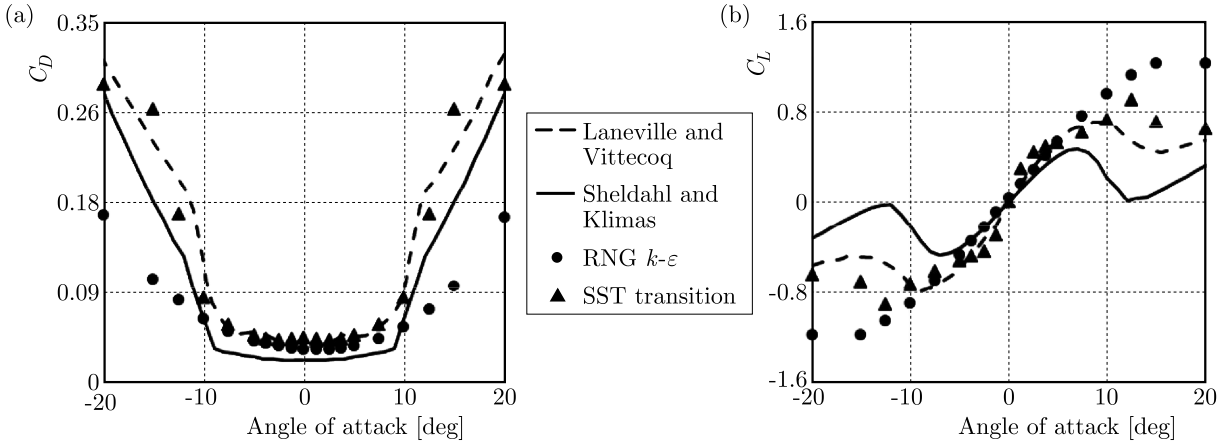

Fig. 7. (a) Drag and (b) lift force coefficients versus the angle of attack

6. Conclusions

The main purposes of this paper are the investigation of steady and unsteady lift and drag coefficients of NACA 0018 airfoil using the same mesh distribution around the airfoil and two turbulence models: the RNG k-ε and the SST Transition. The analysis shows that:

- For the same mesh around the airfoils, consisting of structural quadrilateral elements near the blades and triangle elements elsewhere, the steady airfoil characteristics are in good agreement with the experimental results. However, 3D effects may cause errors in the experiment.
- The SST Transition turbulence model gives more realistic results of aerodynamic force coefficients than the RNG k-ε model.
- Comparison of the results of the lift force coefficient obtained during two independent experiments shows significant differences in the static stall zones.

This paper gives some preliminary results of steady RANS modeling of the flow past a turbine rotor. The presented simulations are a part of a more extensive numerical study of vertical-axis wind turbines. The results of simulations presented in the paper can be a database for other investigations.

Acknowledgments

This work has been supported by the European Union in the framework of European Social Fund through the "Didactic Development Program of the Faculty of Power and Aeronautical Engineering of the Warsaw University of Technology".

References

1. Akimoto H., Hara Y., Kawamura T., Nakamura T., Lee Y.-S., 2013, A conformal mapping technique to correlate the rotating flow around a wing section of vertical axis wind turbine and an equivalent linear flow around a static wing, *Environmental Research Letters*, **8**, 044040
2. Amet E., Maître T., Pellone C., Achard J.-L., 2009, 2D numerical simulations of blade-vortex interaction in a Darrieus turbine, *Journal of Fluids Engineering*, **131**, 111103-1-15
3. Blackwell B.F., 1974, The vertical-axis wind turbine "how it works", Report SLA-74-0160, Sandia Laboratories, USA
4. Borg M., Shires A., Collu M., 2014, Offshore floating vertical axis wind turbines, dynamics modelling state of the art. Part I: Aerodynamics, *Renewable and Sustainable Energy Reviews*, **39**, 1214-1225
5. Danao L.A., Qin N., Howell R., 2012, A numerical study of blade thickness and camber effects on vertical axis wind turbines, *Proceedings of the Institution of Mechanical Engineers, Part A: Journal of Power and Energy*, **226**, 7, 867-881
6. Ferreira C., 2009, The near wake of the VAWT: 2D and 3D views of the VAWT aerodynamics, Ph.D. Thesis, Delft University of Technology
7. Ferreira C., van Bussel G., van Kuik G., 2007, 2D CFD simulation of dynamic stall on a Vertical Axis Wind Turbine: verification and validation with PIV measurements, *45th AIAA Aerospace Sciences Meeting and Exhibit/ASME Wind Energy Symposium*, Reno, 16191-16201
8. Ferreira C., van Bussel G.W., van Kuik G.M., Scarano F., 2011, On the use of velocity data for load estimation of a VAWT in dynamic stall, *Journal of Solar Energy Engineering*, **133**, 1, 011006-011006-8
9. Hansen M.O.L., 2008, *Aerodynamics of Wind Turbines*, Second Edition, Earthscan
10. Hau E., 2006, *Wind Turbines*, Springer
11. Laneville A., Vittecoq P., 1986, Dynamic stall: the case of the vertical axis wind turbine, *Journal of Solar Energy Engineering*, **108**, 141-145
12. Lichota P., 2013, Maximum Likelihood estimation: a method for flight dynamics – angle of attack estimation, *14th International Carpathian Control Conference, IEEE*, Rytro, Poland, 218-221

13. Lichota P., 2016, Inclusion of the D-optimality in multisine manoeuvre design for aircraft parameter estimation, *Journal of Theoretical and Applied Mechanics*, **54**, 1, 87-98

14. Madsen H., Larsen T., Vita L., Paulsen U., 2013, Implementation of the actuator cylinder flow model in HAWC2 for aeroelastic simulations on vertical axis wind turbines, *51st AIAA Aerospace Sciences Meeting Including the New Horizons Forum and Aerospace Exposition*, Texas, USA

15. Maroński R., 2016, *Wind Turbines* (in Polish), Oficyna Wydawnicza Politechniki Warszawskiej, Warszawa

16. Marsh P., Ranmuthugala D., Penesis I., Thomas G., 2013, Performance predictions of a straight-bladed vertical axis turbine using double-multiple streamtube and computational fluid dynamics models, *Journal of Ocean Technology*, **8**, 1, 87-103

17. Paraschivoiu I., 2009, *Wind Turbine Design with Emphasis on Darrieus Concept*, Presses Internationales Polytechnique

18. Ponta F.L., Jacovkis P.M., 2001, A vortex model for Darrieus turbine using finite element techniques, *Renewable Energy*, **24**, 1, 1-18

19. Rogowski K., 2014, Analysis of performance of the Darrieus wind turbine, Ph.D. Thesis, Warsaw University of Technology, Faculty of Power and Aeronautical Engineering, Warsaw

20. Rogowski K., Maroński R., 2015, CFD computation of the Savonius rotor, *Journal of Theoretical and Applied Mechanics*, **53**, 1, 37-45

21. Sarlak H., Mikkelsen R., Sarmast S., Sørensen J.N., 2014, Aerodynamic behaviour of NREL S826 airfoil at Re=100,000, *Journal of Physics: Conference Series*, **524**, 1

22. Scheurich F., Fletcher T.M., Brown R.E., 2011. Simulating the aerodynamic performance and wake dynamics of a vertical-axis wind turbine, *Wind Energy*, **14**, 159-177

23. Sheldahl R.E., Klimas P.C., 1981, Aerodynamic characteristics of seven symmetrical airfoil sections through 180-degree angle of attack for use in aerodynamic analysis of vertical axis wind turbines, Energy Report SAND80-2114, Sandia National Laboratories, Albuquerque, New Mexico

24. Strickland J.H., Smith T., Sun K., 1981, A vortex model of the Darrieus turbine: an analytical and experimental study, Sandia National Laboratories, Technical Report SAND 81-7017

25. Strickland J.H., Webster B.T., Nguyen T., 1979, A vortex model of the Darrieus turbine: an analytical and experimental study, *Journal of Fluids Engineering*, **101**, 500-505

Manuscript received July 27, 2017; accepted for print August 31, 2017